INTERNATIONAL JOURNAL FOR NUMERICAL AND ANALYTICAL METHODS IN GEOMECHANICS

The Role of Nonlinear Hardening/Softening in Probabilistic Elasto-Plasticity

Kallol Sett, Boris Jeremić*and M. Levent Kavvas

Department of Civil and Environmental Engineering, University of California, Davis, CA 95616

Accepted for publication

1. ABSTRACT

The elastic–plastic modeling and simulations have been studied extensively in the last century. However, one crucial area of material modeling has received very little attention. The uncertainties in material properties probably have the largest influence on many aspects of structural and solids behavior. Despite its importance, effects of uncertainties of material properties on overall response of structures and solids have rarely been studied. Most of the small number of studies on effects of material variabilities have used repetitive deterministic models through Monte–Carlo type simulations. While this approach might appear sound,

*Correspondence to: Boris Jeremić, Department of Civil and Environmental Engineering, University of California, One Shields Ave., Davis, CA 95616, jeremic@ucdavis.edu

it cannot be both computationally efficient and statistically accurate (have statistically appropriate number of data points).

Recently, we have developed a methodology to solve the probabilistic elastic–plastic differential equations. The methodology is based on Eulerian–Lagrangian form of the Fokker–Planck–Kolmogorov equation and provides for full description of the probability density function (PDF) of stress response for a given strain.

In this paper we describe our development in some details. In particular, we investigate the effects of nonlinear hardening on predicted PDF of stress. As it will be shown, the nonlinear hardening will create a discrepancy between the most likely stress solution and the deterministic solution. This discrepancy, in fact, means that the deterministic solution is not the most likely outcome of the corresponding probabilistic solution if material parameters are uncertain (and they always are, we just tend to simplify that fact and use, for example, mean values for deterministic simulations).

A number of examples will be presented, illustrating methodology and main results, some of which are quite surprising as mentioned above.

KEY WORDS: Elasto-Plasticity, Probability Theory, Fokker-Planck-Kolmogorov Equation

2. INTRODUCTION

Numerical simulations of mechanical behavior of solids and structures made of geomaterials are inherently uncertain. The natural conditions with which geotechnical engineers deal with are unknown and must be inferred from limited and expensive observations (Beacher and Christian

[2]). For example Fig. 1 shows measured soil properties in Mexico City. Large variability

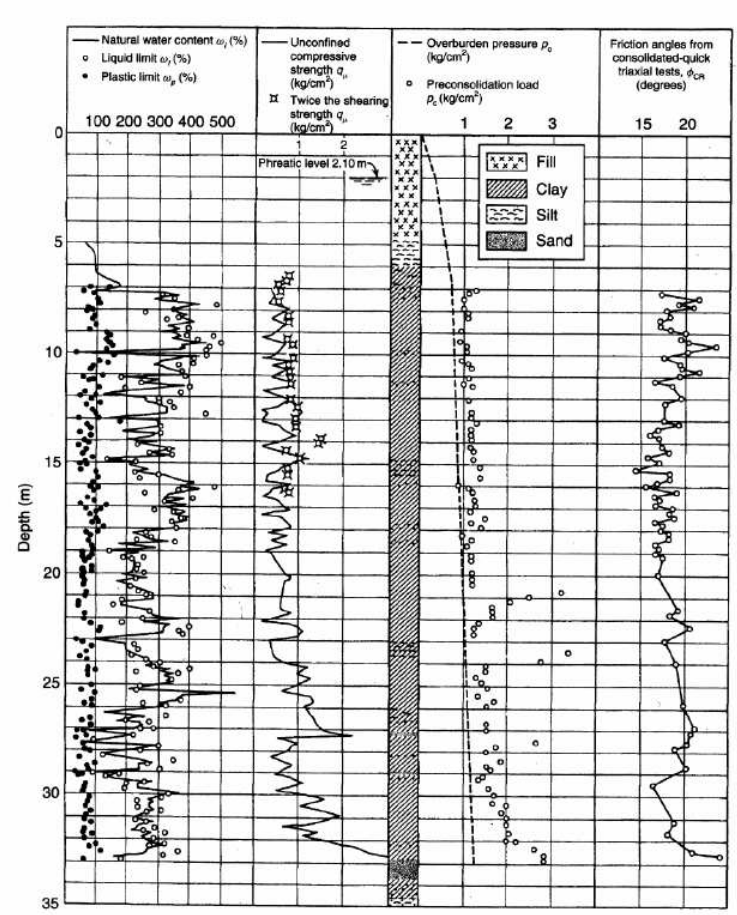

Figure 1. Measured values of mechanical properties of soil from Mexico city, typical soft spot (after Baecher and Christian [2]

in material properties can be noted as a function of depth. It is important to note that this soil formation is considered very homogeneous (Baecher and Christian [2]). The usual procedure in this case is to choose either constant properties or fit smooth (usually linear) curves to properties of interest (for example friction angle and/or unconfined compressive strength and/or preconsolidation pressure (refer Fig. 1)) and use the assumed (much simplified)

properties in modeling and simulations related to this soil profile. This approach will completely neglect the variations which might have a large effect on response of this soil profile. The usual remedy is to apply a large factor of safety, which, it is hoped, will cover up for neglected information. Use of large factors of safety is becoming unacceptable as it leads to design solutions that are not only uneconomical but also sometimes not even safe (Duncan [4]). More appropriate methods for analyzing the random fields of material properties have been described by Ghanem and Spanos [9], Matthies and Keese [13], Roberts and Spanos [17], Zhu et al, [24], Soize [19].

In recent years, civil engineering practice, and particularly geotechnical engineering practice has seen an increasing emphasis on quantification of uncertainties. Quantifications or mathematical descriptions of uncertainties are usually done within the framework of probability theory, where random soil parameters are modeled as random variables (if they are specialized to a fixed location in the domain) or random fields (if they are specialized to the function of location in the domain). Nice descriptions of different types of soil parameter uncertainties and their quantification methods were presented by Phoon & Kulhawy ([15], [16]) and Fenton ([5], [6]). The uncertainty in G/G_{max} curve was recently quantified by Stokoe et al. [20].

Even-though there is a widely acknowledged necessity to model soil properties using theory of probability, there is very little work on propagation of uncertainties in soil properties through elastic–plastic constitutive equation. Advanced elasto–plasticity based constitutive models, when properly calibrated, although very accurate, are, in general, highly sensitive to fluctuations in model parameters (cf. Borja [3]). In the field of geomechanics, this sensitivity aspect of constitutive model is of great importance as the uncertainties associated with soil properties could outweigh the advantages gained by advanced and sophisticated models.

First attempt to propagate randomness through the elastic–plastic constitutive equations, considering random Young's modulus was published only recently by Anders and Hori [1]. They based their work on perturbation expansion at the stochastic mean behavior. In computing the mean behavior they took advantage of bounding media analysis. However, because of the use of Taylor series expansion, this approach is limited to problems with small coefficients of variation. According to a recent report by Sudret and Der Kiureghian [21], the coefficient of variation should not exceed 20 % if this approach is to be used. This limitation restricts the use of perturbation method to general geomechanics problems, where the coefficients of variation of soil properties are rarely less than 20% (eg. Phoon and Kulhawy [15]). Another disadvantage of the perturbation method is that it inherits the so-called "closure problem" (cf. Kavvas [11]), where information on higher–order moments is always needed to calculate lower–order moments. More recently, Fenton and Griffiths [7] used a Monte–Carlo type method to propagate uncertainties through elastic–plastic $c - \phi$ soil.

Conventional Monte–Carlo simulation, although very accurate, might be computationally expensive for general elastic–plastic simulations. The method typically requires a statistically appropriate number of realizations per random variable (often a very large number) in order to satisfy statistical accuracy. This repetitive use of computationally expensive deterministic model renders the Monte–Carlo simulation impractical. Monte–Carlo simulations, however, find a great use in verification of analytical developments (cf. Oberkampf et al, [14]).

In order to overcome the drawbacks associated with Monte–Carlo technique and perturbation method in dealing with non-linear stochastic differential equations (SDEs), Kavvas [11] derived a generic Eulerian-Lagrangian form of Fokker–Planck–Kolmogorov equation (FPKE) for the second–order exact probabilistic solution of any non-linear ODE with

stochastic coefficient and stochastic forcing. The development was focusing on applications in water resources engineering but, it is general enough to apply to any non-linear ODE with stochastic coefficient and stochastic forcing. Using the above mentioned Eulerian–Lagrangian form of FPKE, Jeremić et al. [10] and Sett et al. [18] recently developed formulation and solution for the general 1-D elastic-plastic constitutive rate equation with random material properties and random strain rate.

The main advantage of FPKE-based approach is that a complete probabilistic description (probability density function (PDF)) of stress can be obtained exactly to second-order accuracy (to covariance of time), given random material property(ies) and/or random strain. In addition to that, even if the FPKE is not solvable in closed-form solution, the deterministic linearity of the FPKE in terms of the state variable, the probability density of stress, considerably simplifies the numerical solution process.

In this paper we present a general expression, in the form of a partial differential equation, for evolution of the probability density of stress with strain for any general 3-D point-location scale/local-average form of elastic-plastic constitutive law with material properties and strain rate modeled as random variables/fields. The expression for the PDF of stress is developed in a general way, making it usable in any dimension (1–,2– or 3–D) and for any type of incremental elastic–plastic material model. Application of the developed methodology is demonstrated through 1-D point-location scale Cam-Clay shear constitutive law. In particular, the effects of non–linear hardening and softening on the predicted PDFs of stresses are investigated.

3. GENERAL EXPRESSION FOR 3–D PROBABILISTIC CONSTITUTIVE RATE EQUATION IN LOCAL-AVERAGE FORM

The incremental form of spatial-average 3-D elastic-plastic constitutive rate equation can be written as:

$$\frac{d\sigma_{ij}(x_t,t)}{dt} = D^{ep}_{ijkl}(\sigma_{ij}, D^{el}_{ijkl}, f, U, q_*, r_*; x_t, t)\frac{d\epsilon_{kl}(x_t,t)}{dt} \tag{1}$$

where, D^{ep}_{ijkl} is the *random, non-linear elastic-plastic coefficient tensor* which is a function of random stress tensor (σ_{ij}), random elastic moduli tensor (D^{el}_{ijkl}), random yield function (f), random potential function (U), random internal variables (q_*) and random direction of evolution of internal variables (r_*). The random internal variables (q_*) could be scalar (for perfectly plastic and isotropic hardening models), or second-order tensor (for translational and rotational kinematic hardening models), or fourth-order tensor (for distortional hardening models) or any combinations of the above. The same classification applies to the random direction of evolution of internal variables (r_*). By denoting all the random material parameters by a parameter tensor as:

$$D_{ijkl} = \left[D^{el}_{ijkl}, f, U, q_*, r_*\right] \tag{2}$$

and introducing a random operator tensor, η_{ij}, one can write Eq. (1) as,

$$\frac{d\sigma_{ij}(x,t)}{dt} = \eta_{ij}(\sigma_{ij}, D_{ijkl}, \epsilon_{kl}; x, t) \tag{3}$$

with an initial condition,

$$\sigma_{ij}(x,0) = \sigma_{ij_0} \tag{4}$$

In Eq. (3), the stress tensor σ_{ij} can be considered to represent a point in a 9-dimensional stress (σ)-space and hence Eq. (3) determines the velocity for the point in this space. It is possible to visualize this, by imagining an initial point in stress space, given by its initial

condition σ_{ij_0}, with a trajectory starting out that describes the corresponding solution of the non-linear stochastic ordinary differential equation (ODE) system (Eq. (3)). Let us now consider a cloud of initial points, described by a density $\rho(\sigma_{ij}, 0)$ in the σ-space, and with movements of these points dictated by Eq. (3), the phase density ρ of $\sigma_{ij}(x,t)$ varies in time according to a continuity equation which expresses the conservation of all these points in the σ-space.

Expressing this continuity equation in mathematical terms, one obtains Kubo's stochastic Liouville equation (Kubo [12]):

$$\frac{\partial \rho(\sigma_{ij}(x,t),t)}{\partial t} = -\frac{\partial}{\partial \sigma_{mn}} \eta_{mn} \left(\sigma_{mn}(x,t), D_{mnpq}(x), \epsilon_{pq}(x,t)\right) \rho(\sigma_{ij}(x,t),t) \tag{5}$$

with initial condition,

$$\rho(\sigma_{ij}, 0) = \delta(\sigma_{ij} - \sigma_{ij_0}) \tag{6}$$

where $\delta(\cdot)$ is the Dirac delta function. Eq. (6) is the probabilistic restatement in the σ-phase space of the original deterministic initial condition (Eq. (4)). One can then apply Van Kampen's Lemma (Van Kampen [22]) to obtain:

$$< \rho(\sigma_{ij}, t) >= P(\sigma_{ij}, t) \tag{7}$$

where, the symbol $< \cdot >$ denotes the expectation operation, and $P(\sigma_{ij}, t)$ denotes evolutionary probability density of the state variable tensor σ_{ij} from the constitutive equations.

Therefore, in order to obtain the multivariate probability density function (PDF), $P(\sigma_{ij}, t)$, of the state variable tensor σ_{ij}, it is necessary to obtain the deterministic partial differential equation (PDE) of the σ-space mean phase density $< \rho(\sigma_{ij}, t) >$ from the linear stochastic PDE system (Eqs. (5) and (6)). This necessitates the derivation of the ensemble average form of Eq. (5) for $< \rho(\sigma_{ij}, t) >$. The ensemble average form of Eq. (5) was derived by Kavvas [11]

as follows:

$$\begin{aligned}\frac{\partial \langle \rho(\sigma_{ij}(x_t,t),t)\rangle}{\partial t} &= -\frac{\partial}{\partial \sigma_{mn}}\left[\left\{\left\langle \eta_{mn}(\sigma_{mn}(x_t,t), D_{mnrs}(x_t), \epsilon_{rs}(x_t,t))\right\rangle\right.\right.\\ &- \int_0^t d\tau Cov_0\left[\eta_{mn}(\sigma_{mn}(x_t,t), D_{mnrs}(x_t), \epsilon_{rs}(x_t,t));\right.\\ &\left.\left.\left.\frac{\partial \eta_{ab}(\sigma_{ab}(x_{t-\tau},t-\tau), D_{abcd}(x_{t-\tau}), \epsilon_{cd}(x_{t-\tau},t-\tau)}{\partial \sigma_{ab}}\right]\right\}\langle \rho(\sigma_{ij}(x_t,t),t)\rangle\right]\\ &+ \frac{\partial}{\partial \sigma_{mn}}\left[\left\{\int_0^t d\tau Cov_0\left[\eta_{mn}(\sigma_{mn}(x_t,t), D_{mnrs}(x_t), \epsilon_{rs}(x_t,t));\right.\right.\right.\\ &\left.\left.\left.\eta_{ab}(\sigma_{ab}(x_{t-\tau},t-\tau), D_{abcd}(x_{t-\tau}), \epsilon_{cd}(x_{t-\tau},t-\tau))\right]\right\}\frac{\partial \langle \rho(\sigma_{ij}(x_t,t),t)\rangle}{\partial \sigma_{ab}}\right] \qquad (8)\end{aligned}$$

to exact second order (to the order of the covariance time of η). In Eq. (8), $Cov_0[\cdot]$ is the time ordered covariance function defined by,

$$Cov_0\left[\eta_{mn}(x,t_1), \eta_{ab}(x,t_2)\right] = \langle \eta_{mn}(x,t_1)\eta_{ab}(x,t_2)\rangle - \langle \eta_{mn}(x,t_1)\rangle \cdot \langle \eta_{ab}(x,t_2)\rangle \qquad (9)$$

By combining Eq. (8) with Eq. (7) and rearranging the terms yields the following Eulerian-Lagrangian form of Fokker–Planck–Kolmogorov equation (FPKE) (cf. Kavvas [11]):

$$\begin{aligned}\frac{\partial P(\sigma_{ij}(x_t,t),t)}{\partial t} &= \frac{\partial}{\partial \sigma_{mn}}\left[\left\{\left\langle \eta_{mn}(\sigma_{mn}(x_t,t), D_{mnrs}(x_t), \epsilon_{rs}(x_t,t))\right\rangle\right.\right.\\ &+ \int_0^t d\tau Cov_0\left[\frac{\partial \eta_{mn}(\sigma_{mn}(x_t,t), D_{mnrs}(x_t), \epsilon_{rs}(x_t,t))}{\partial \sigma_{ab}};\right.\\ &\left.\left.\left.\eta_{ab}(\sigma_{ab}(x_{t-\tau},t-\tau), D_{abcd}(x_{t-\tau}), \epsilon_{cd}(x_{t-\tau},t-\tau)\right]\right\}P(\sigma_{ij}(x_t,t),t)\right]\\ &+ \frac{\partial^2}{\partial \sigma_{mn}\partial \sigma_{ab}}\left[\left\{\int_0^t d\tau Cov_0\left[\eta_{mn}(\sigma_{mn}(x_t,t), D_{mnrs}(x_t), \epsilon_{rs}(x_t,t));\right.\right.\right.\\ &\left.\left.\left.\eta_{ab}(\sigma_{ab}(x_{t-\tau},t-\tau), D_{abcd}(x_{t-\tau}), \epsilon_{cd}(x_{t-\tau},t-\tau))\right]\right\}P(\sigma_{ij}(x_t,t),t)\right] \qquad (10)\end{aligned}$$

to exact second order. The solution of this deterministic linear FPKE (Eq. (10)) in terms of $P(\sigma_{ij},t)$ under appropriate initial and boundary conditions will yield the PDF of the state variable tensor σ_{ij}. It is important to note that while the original equation (Eq. (1)) is non-linear, the FPKE (Eq. (10)) is linear in terms of its unknown, the probability density $P(\sigma_{ij},t)$

of the state variable tensor σ_{ij}. This linearity, in turn, provides significant advantages in probabilistic solution of the constitutive rate equation.

One should also note that Eq. (10) is a mixed Eulerian-Lagrangian equation, since, while the real space location x_t at time t is known, the location $x_{t-\tau}$ is an unknown. If one assumes, for example, small strain theory, one can relate the unknown location $x_{t-\tau}$ from the known location x_t by using the strain rate, $\dot{\epsilon}$ $(=d\epsilon/dt)$ as,

$$d\epsilon = \dot{\epsilon}\tau = \frac{x_t - x_{t-\tau}}{x_t} \tag{11}$$

or, by rearranging

$$x_{t-\tau} = (1 - \dot{\epsilon}\tau)x_t \tag{12}$$

Another interesting aspect to note, possibly of theoretical interest, is the Itô stochastic differential equation (SDE) form of the constitutive rate equation with random material properties and random strain rate (Eq. (3)). Utilizing the connection between FPKE and Itô SDE (cf. Gardiner [8]), one can write Eq. (10) as:

$$\begin{aligned} d\sigma_{ij}(x,t) = & \\ & \left\{ \left\langle \eta_{ij}(\sigma_{ij}(x_t,t), D_{ijkl}(x_t), \epsilon_{kl}(x_t,t)) \right\rangle + \int_0^t d\tau Cov_0 \left[\frac{\partial \eta_{ij}(\sigma_{ij}(x_t,t), D_{ijkl}(x_t), \epsilon_{kl}(x_t,t))}{\partial \sigma_{ab}}; \right.\right. \\ & \left.\left. \eta_{ab}(\sigma_{ab}(x_{t-\tau}, t-\tau), D_{abcd}(x_{t-\tau}), \epsilon_{cd}(x_{t-\tau}, t-\tau)) \right] \right\} dt + C_{ijm}(\sigma_K, t) dW_m(t) \end{aligned} \tag{13}$$

where,

$$\begin{aligned} C_{ijm}(\sigma_{ij},t) C_{abm}(\sigma_{ab},t) = 2 \int_0^t d\tau Cov_0 \Big[& \eta_{ij}(\sigma_{ij}(x_t,t), D_{ijkl}(x_t), \epsilon_{kl}(x_t,t)); \\ & \eta_{ab}(\sigma_{ab}(x_{t-\tau}, t-\tau), D_{abcd}(x_{t-\tau}), \epsilon_{cd}(x_{t-\tau}, t-\tau)) \Big] \end{aligned} \tag{14}$$

and, $dW_i(t)$ is an increment of the vector Wiener process W_i having the following properties:

$$< dW_i(t) >= 0 \tag{15}$$

and,

$$\begin{aligned} < dW_i(t)dW_j(t) > &= \delta_{ij}dt \ \text{ for } \tau = t \\ &= 0 \ \text{ for } \tau \neq t \end{aligned} \tag{16}$$

It is also interesting to note that all the stochasticity of the original system of equations (Eq. (3)) are lumped together in the last term (Wiener increment term) of the r.h.s of Eq. (13).

In theory, one could use the Itô form of the constitutive rate equation (Eq. (13)) in obtaining the mean of stress tensor (σ_{ij}) as (cf. Kavvas [11]):

$$\begin{aligned} &\frac{< d\sigma_{ij}(x,t) >}{dt} = \\ &\left\langle \eta_{ij}(\sigma_{ij}(x_t,t), D_{ijkl}(x_t), \epsilon_{kl}(x_t,t)) \right\rangle + \int_0^t d\tau Cov_0 \Bigg[\frac{\partial \eta_{ij}(\sigma_{ij}(x_t,t), D_{ijkl}(x_t), \epsilon_{kl}(x_t,t))}{\partial \sigma_{ab}}; \\ &\eta_{ab}(\sigma_{ab}(x_{t-\tau}, t-\tau), D_{abcd}(x_{t-\tau}), \epsilon_{cd}(x_{t-\tau}, t-\tau)) \Bigg] \end{aligned} \tag{17}$$

but the difficulty is that the stress tensor appearing within $\eta_{ij}(\cdot)$ in the covariance term on the r.h.s of Eq. (17) is random and needs to be treated accordingly. One possible way is perturbation with respect to mean, however the "closure problem" (cf. Kavvas [11]) will make this type of solution problematic. Hence in this study the mean of stress tensor (σ_{ij}) will be computed by standard operation on the PDF of stress tensor (σ_{ij}), which will be obtained by solving the Fokker–Planck–Kolmogorov PDE (Eq. (10)).

4. APPLICATION TO PROBABILISTIC BEHAVIOR OF 1-D CAM–CLAY ELASTIC-PLASTIC CONSTITUTIVE EQUATION

In this section the applicability of the presented general expression in obtaining PDF and subsequently mean and variance behaviors of stress will be demonstrated for 1-D, elastic–plastic, Cam–Clay constitutive rate equation. The general incremental form of constitutive

equation with single scalar internal variable can be written as:

$$\frac{d\sigma_{ij}(t)}{dt} = D^{ep}_{ijkl}(t)\frac{d\epsilon_{kl}(t)}{dt} \tag{18}$$

where the stiffness tensor D^{ep}_{ijkl} is given as:

$$D^{ep}_{ijkl} = \begin{cases} D^{el}_{ijkl} & \text{when} \quad f < 0 \vee (f = 0 \wedge df < 0) \\ D^{el}_{ijkl} - \dfrac{D^{el}_{ijmn}\dfrac{\partial f}{\partial \sigma_{mn}}\dfrac{\partial f}{\partial \sigma_{pq}}D^{el}_{pqkl}}{\dfrac{\partial f}{\partial \sigma_{rs}}D^{el}_{rstu}\dfrac{\partial f}{\partial \sigma_{tu}} - \dfrac{\partial f}{\partial p_0}\bar{p}_0} & \text{when} \quad f = 0 \vee df = 0 \end{cases} \tag{19}$$

where D^{el}_{ijkl} is the elastic stiffness tensor and D^{ep}_{ijkl} is the elastic–plastic stiffness tensor. The internal variable p_0 in this case depends on plastic volumetric strain and has a physical meaning (for Cam–Clay) as the maximum hydrostatic stress the soil has experienced during previous loading history). It was assumed that the material obeys associative flow rule (as is it is usually assumed for Cam–Clay material model). Hence, both the yield and the plastic potential functions f are given by (Cam–Clay material model):

$$f = \hat{f}(p, q) = p^2 - p_0 p + \frac{q^2}{M^2} = 0 \tag{20}$$

Material parameter M represents the slope of the critical state line in the $p - q$ space. The stress invariants p and q are given as:

$$p = -\frac{\sigma_{kk}}{3} = -\frac{\sigma_{11} + \sigma_{22} + \sigma_{33}}{3} \tag{21}$$

$$q = \sqrt{\frac{3}{2}s_{ij}s_{ij}} = \frac{1}{\sqrt{2}}\left[(\sigma_{11} - \sigma_{22})^2 + (\sigma_{22} - \sigma_{33})^2 + (\sigma_{33} - \sigma_{11})^2 + 6\sigma_{12}^2 + 6\sigma_{23}^2 + 6\sigma_{31}^2\right]^{1/2} \tag{22}$$

One can work on components of the Eq. 19 to obtain:

$$A_{kl} = \frac{\partial f}{\partial \sigma_{pq}} D^{el}_{pqkl} = \frac{\partial f}{\partial p}\left[2G\left(\frac{\partial p}{\partial \sigma_{11}}\delta_{1l}\delta_{1k} + \frac{\partial p}{\partial \sigma_{22}}\delta_{2l}\delta_{2k} + \frac{\partial p}{\partial \sigma_{33}}\delta_{3l}\delta_{3k}\right) + \left(K - \frac{2}{3}G\right)\frac{\partial p}{\partial \sigma_{cd}}\delta_{cd}\delta_{kl}\right] + \frac{\partial f}{\partial q}\left[2G\frac{\partial q}{\partial \sigma_{ij}}\delta_{ik}\delta_{jl} + \left(K - \frac{2}{3}G\right)\frac{\partial q}{\partial \sigma_{ab}}\delta_{ab}\delta_{kl}\right] \tag{23}$$

and

$$B = \frac{\partial f}{\partial \sigma_{rs}} D^{el}_{rstu} \frac{\partial f}{\partial \sigma_{tu}} = \left(\frac{\partial f}{\partial p}\right)^2\left[2G\left\{\left(\frac{\partial p}{\partial \sigma_{11}}\right)^2 + \left(\frac{\partial p}{\partial \sigma_{22}}\right)^2 + \left(\frac{\partial p}{\partial \sigma_{33}}\right)^2\right\} + \left(K - \frac{2}{3}G\right)\left\{\frac{\partial p}{\partial \sigma_{ij}}\delta_{ij}\right\}^2\right] + \left(\frac{\partial f}{\partial q}\right)^2\left[2G\frac{\partial q}{\partial \sigma_{ij}}\frac{\partial q}{\partial \sigma_{ij}} + \left(K - \frac{2}{3}G\right)\left\{\frac{\partial q}{\partial \sigma_{ij}}\delta_{ij}\right\}^2\right] \tag{24}$$

where, K and G are the elastic bulk and shear modulus, respectively. For the Cam–Clay formulation the material parameter p_0 represents an internal variable and its evolution depends on the plastic volumetric strain. Hence, the plastic modulus K_P becomes:

$$K_P = -\frac{\partial f}{\partial p_0}\bar{p}_0 = (1 + e_0)\frac{p_0}{\lambda - \kappa}\frac{\partial f}{\partial p} \tag{25}$$

One may note that the differentiations appearing in Eqs. (23), (24), and (25), involve stochastic process and hence cannot be carried out in a deterministic sense. Substituting Eqs. (23), (24), and (25) into (19) one may obtain the random operator tensor (η_{ij}) specialized to Cam–Clay model as:

$$\eta_{ij} = \begin{cases} \left[2G\delta_{ik}\delta_{jl} + \left(K - \frac{2}{3}G\right)\delta_{ij}\delta_{kl}\right]\frac{d\epsilon_{kl}}{dt} & \text{when} \quad f < 0 \vee (f = 0 \wedge df < 0) \\ \left[2G\delta_{ik}\delta_{jl} + \left(K - \frac{2}{3}G\right)\delta_{ij}\delta_{kl} - \frac{A_{ij}A_{kl}}{B + K_P}\right]\frac{d\epsilon_{kl}}{dt} & \text{when} \quad f = 0 \vee df = 0 \end{cases} \tag{26}$$

where A_{ij}, B, and K_P are defined by Eqs. (23), (24), and (25) respectively.

Previously developed random operator tensor η_{ij} for Cam–Clay material model will be now specialized to 1-D shear behavior, resulting in the following equation for the PDF of shear stress:

$$\begin{aligned}\frac{\partial P(\sigma_{12}(t),t)}{\partial t} &= -\frac{\partial}{\partial \sigma_{12}}\left[\left\{ \langle \eta(\sigma_{12}(t), D_{1212}, \epsilon_{12}(t))\rangle \right.\right. \\ &+ \int_0^t d\tau Cov_0\left[\frac{\partial \eta(\sigma_{12}(t), D_{1212}, \epsilon_{12}(t))}{\partial \sigma_{12}}; \eta(\sigma_{12}(t-\tau), D_{1212}, \epsilon_{12}(t-\tau)\Big)\right]\right\} P(\sigma_{12}(t),t)\Big] \\ &+ \frac{\partial^2}{\partial \sigma_{12}^2}\left[\left\{\int_0^t d\tau Cov_0\left[\eta(\sigma_{12}(t), D_{1212}, \epsilon_{12}(t)); \eta\sigma_{12}(t-\tau), D_{1212}, \epsilon_{12}(t-\tau)\right]\right\} P(\sigma_{12}(t),t)\right]\end{aligned} \tag{27}$$

One may note that while solving Eq. (27) for probability density ($P(\sigma_{12})$) of each fixed value of σ_{12} in its domain, the σ_{12} terms appearing within $\eta(\cdot)$ are deterministic and hence the differentiations involving σ_{12} can be carried out in a usual sense. In Eq. (27) the random operator function η is different for pre–yield (elastic) and post–yield (elastic–plastic) responses. For pre–yield, linear elastic response, one can obtain the random operator function η in the form:

$$\eta = 2G\frac{d\epsilon_{12}}{dt} \tag{28}$$

while, for post-yield, non-linear, elastic–plastic response η obtains the form:

$$\eta = \left[2G - \frac{\left(36\frac{G^2}{M^4}\right)\sigma_{12}^2}{\frac{(1+e_0)p\left(p-\frac{3\sigma_{12}^2}{pM^2}\right)^2}{\kappa} + \left(18\frac{G}{M^4}\right)\sigma_{12}^2 + \frac{1+e_0}{\lambda-\kappa}pp_0\left(p-\frac{3\sigma_{12}^2}{pM^2}\right)}\right]\frac{d\epsilon_{12}}{dt} \tag{29}$$

5. RESULTS AND DISCUSSIONS

In this section the Fokker–Planck–Kolmogorov (FPK) equation is solved using appropriate initial and boundary conditions. The FPK equation is specialized to 1-D (shear) Cam–Clay constitutive relationship with different degrees of uncertainties (Eqs. (27), (28), and (29)) and the solution will be in terms of the evolution of Probability Density Function (PDF) of shear stress (σ_{12}) with time (and/or strain), given random material property(ies) and deterministic shear strain. It should be noted that the strain can be random as well, and the equations can be solved in that case too, but for the sake of simplicity, strain (or time) is preset to deterministic value. In other words, the solution is driven by deterministic strain.

5.1. Initial and Boundary Conditions

The Fokker–Planck–Kolmogorov PDE specialized to 1–D Cam–Clay shear constitutive rate equation (Eq. (27) can be written in the following simplified form:

$$\begin{aligned}\frac{\partial P(\sigma_{12},t)}{\partial t} &= -\frac{\partial}{\partial \sigma_{12}}\left\{P(\sigma_{12},t)N_{(1)}\right\}+\frac{\partial^2}{\partial \sigma_{12}^2}\left\{P(\sigma_{12},t)N_{(2)}\right\} \\ &= -\frac{\partial}{\partial \sigma_{12}}\left[P(\sigma_{12},t)N_{(1)}-\frac{\partial}{\partial \sigma_{12}}\left\{P(\sigma_{12},t)N_{(2)}\right\}\right] \qquad (30)\\ &= -\frac{\partial \zeta}{\partial \sigma_{12}} \qquad (31)\end{aligned}$$

where, $N_{(1)}$ and $N_{(2)}$ are coefficients of the Fokker–Planck–Kolmogorov PDE (Eq. (27)) and represent the expressions within the curly braces of the first and second term respectively on the right hand side of Eq. (27). They are called the advection and diffusion coefficients, respectively as the form of Eq. (27) closely resembles advection-diffusion equation (cf. Gardiner [8]). The symbol ζ in Eq. (31) can be considered to be the probability current (cf. Gardiner [8]), since Eq. (31) is a continuity equation and the state variable of the equation (Eq. (31))

is probability density.

The initial condition for pre-yield (elastic) solution for PDF of shear stress, will be deterministic i.e. at time $t = 0$ all the probability mass is concentrated at $\sigma_{12} = 0$ or at some fixed value of σ_{12} (if there was some initial deterministic stress to begin with). Mathematically, this is represented using Dirac delta function $\delta(\cdot)$,

$$P(\sigma_{12}, 0) = \delta(\sigma_{12}) \tag{32}$$

On the other hand, for solving for post-yield (elastic–plastic) PDF of shear stress, the initial condition will be represented by the PDF of shear stress corresponding to the pre–yield solution (PDF of shear stress at yield).

The initial probability mass, dictated by Eq. (27), will advect and diffuse into the domain of the system throughout the evolution of the simulation. As for the boundary condition, a reflecting barrier boundary is chosen since conservation of the probability mass within the system is required (i.e. no leaking is allowed at the boundaries). Mathematically this condition is expressed as (cf. Gardiner [8])

$$\zeta(\sigma_{12}, t)|_{AtBoundaries} = 0 \tag{33}$$

By making the assumption that the material parameters are normally distributed, theoretically the domain of stress could be from -∞ to +∞ and hence one can write the boundary conditions as:

$$\zeta(-\infty, t) = \zeta(\infty, t) = 0 \tag{34}$$

It should also be noted that any other probabilistic distribution for material parameters can be handled. For example, by assuming that material parameters obey exponential distribution, theoretically the domain of stress could be from 0 to +∞ and hence one can write the boundary

conditions as:

$$\zeta(0,t) = \zeta(\infty,t) = 0 \tag{35}$$

5.2. Numerical Scheme

The FPKE specialized to 1–D Cam–Clay constitutive equation (Eq. (27) with Eqs. (28) or (29)) with initial and boundary conditions (Eqs. (32) and (34) respectively) were solved numerically by *method of lines* (using Mathematica [23]). The Fokker–Planck–Kolmogorov PDE is first semi-discretized into a set of simultaneous ODE systems and then solved by using an ODE solver.

To this end, differentiating by parts the right hand side of Eq. (31) yields:

$$\begin{aligned}\frac{\partial P}{\partial t} &= -N_{(1)}\frac{\partial P}{\partial \sigma_{12}} - P\frac{\partial N_{(1)}}{\partial \sigma_{12}} + N_{(2)}\frac{\partial^2 P}{\partial \sigma_{12}^2} + 2\frac{\partial P}{\partial \sigma_{12}}\frac{\partial N_{(2)}}{\partial \sigma_{12}} + P\frac{\partial^2 N_{(2)}}{\partial \sigma_{12}^2} \\ &= P\left(\frac{\partial^2 N_{(2)}}{\partial \sigma_{12}} - \frac{\partial N_{(1)}}{\partial \sigma_{12}}\right) + \frac{\partial P}{\partial \sigma_{12}}\left(2\frac{\partial N_{(2)}}{\partial \sigma_{12}} - N_{(1)}\right) + \frac{\partial^2 P}{\partial \sigma_{12}^2}N_{(2)}\end{aligned} \tag{36}$$

then, using central difference discretization, as shown in Fig. 2 one can write semi-discretized form of Eq. (36) at any intermediate node i to as:

$$\begin{aligned}\frac{\partial P^{(i)}}{\partial t} = \quad & P^{(i-1)}\left[\frac{N_{(1)}^{(i)}}{2\Delta\sigma_{12}} + \frac{N_{(2)}^{(i)}}{\Delta\sigma_{12}^2} - \frac{1}{\Delta\sigma_{12}}\frac{\partial N_{(2)}^{(i)}}{\partial \sigma_{12}}\right] - P^{(i)}\left[\frac{\partial N_{(1)}^{(i)}}{\partial \sigma_{12}} + 2\frac{N_{(2)}^{(i)}}{\Delta\sigma_{12}^2} - \frac{\partial^2 N_{(2)}^{(i)}}{\partial \sigma_{12}^2}\right] \\ & + P^{(i+1)}\left[-\frac{N_{(1)}^{(i)}}{2\Delta\sigma_{12}} + \frac{N_{(2)}^{(i)}}{\Delta\sigma_{12}^2} + \frac{1}{\Delta\sigma_{12}}\frac{\partial N_{(2)}^{(i)}}{\partial \sigma_{12}}\right]\end{aligned} \tag{37}$$

which forms an initial value problem in the time dimension. It is worth noting that central finite difference technique might not be the most efficient in solving n-dimensional Fokker–Planck–Kolmogorov PDE. Work is underway to improve the efficiency of solution method through adaptivity and reduced order modeling.

It is also noted that, even–though in theory the shear stress (σ_{12}) ranges from -∞ to +∞, for simulation purpose the domain between -0.1 MPa and $+0.1$ MPa is chosen. This choice is

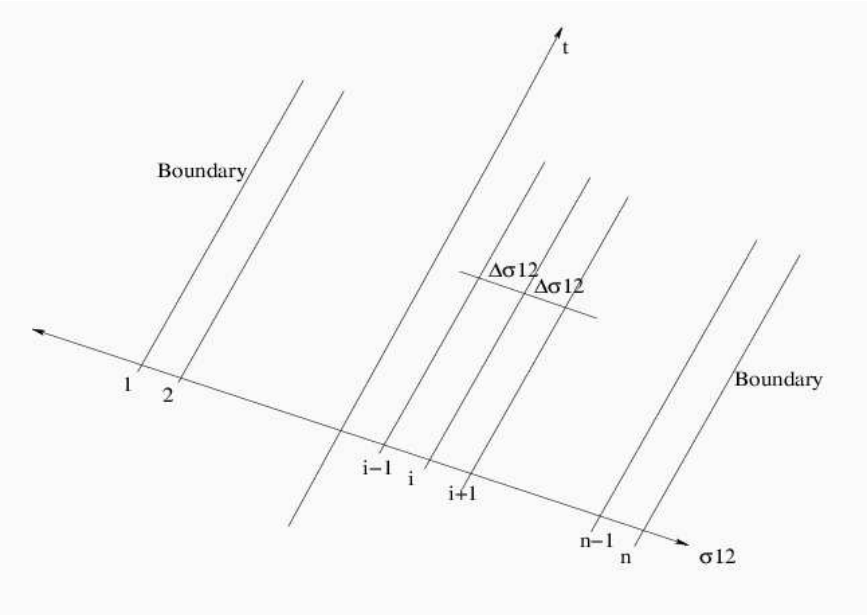

Figure 2. Spatial Discretization of the Fokker–Planck–Kolmogorov PDE

based upon the material properties of the example problem, and by considering the practical range of shear stress (σ_{12}). In addition to that, the Dirac delta function used in initial condition of pre–yield (elastic) solution (Eq. (32)) is numerically approximated using a Gaussian function with zero mean and standard deviation of 0.00001 MPa, as shown in Fig. 3.

While this approximation introduces some error in solution (PDF of shear stress) the error quickly disappears as soon as the solution moves away from the initial condition.

5.3. Simulation Plots

We begin by presenting the results of elastic and elastic–plastic probability density functions for shear stress with only one random material parameter. Fig. 4(a) shows the evolution of probability density function (PDF) of shear stress with time/shear strain for a low over–consolidation ratio (OCR) Cam–Clay material with normally distributed random shear

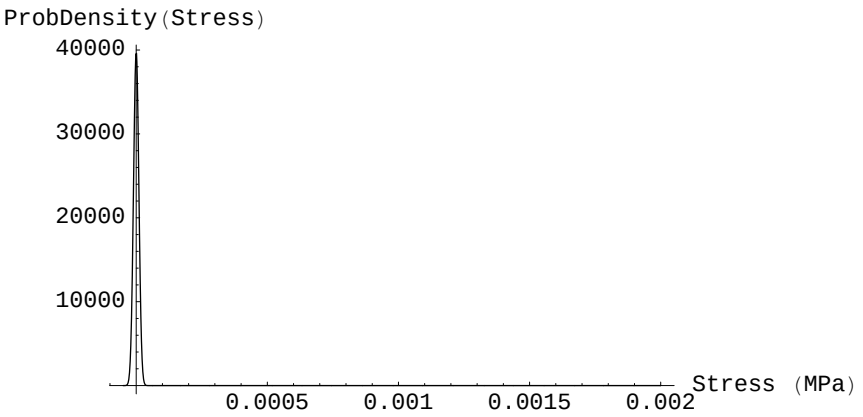

Figure 3. Approximation of Dirac delta Initial Condition (Eq. (32)) with a Gaussian Function of Zero Mean and Standard Deviation of 0.00001 MPa

modulus G (mean value of 2.5 MPa and a standard deviation of 0.5 MPa). The other material properties are considered deterministic and are given as follows: slope of critical state line $M = 0.6$; overconsolidation pressure $p_0 = 0.2$ MPa; applied confinement pressure $p = 0.1$ MPa; slopes of the unloading–reloading and normal compression lines in $e - \ln(p')$ space $\kappa = 0.05$ and $\lambda = 0.25$, respectively; and initial void ratio $e_0 = 2.18$.

As mentioned earlier, the strain is assumed deterministic (strain driven algorithm) while the strain rate is assumed constant ($d\epsilon_{12}/dt$ in Eqs. (28) and (29)). The numerical value of assumed constant strain rate can be substituted in equations (28) and (29) for the entire simulation of the evolution of PDF. As mentioned earlier at the beginning of this section, the FPKE (Eq. (27)) describes the evolution of PDF of shear stress (σ_{12}) with time (t), while the shear strain rate ($d\epsilon_{12}/dt$) describes the evolution of shear strain (ϵ_{12}) with time (t) also. Combining the two, the evolution of PDF of shear stress (σ_{12}) with shear strain (ϵ_{12}) is easily obtained. Time has been brought in this simulation as an intermediate dimension to help in

solution process, and hence, the numerical value of shear strain rate ($d\epsilon_{12}/dt$) could be any arbitrary value. This value of shear strain rate will cancel out once one converts the evolution of PDF of shear stress (σ_{12}) as a function of time, to evolution of PDF of shear stress (σ_{12}) as a function of shear strain (ϵ_{12}). For simulation purpose we assumed the arbitrary value of shear strain rate ($d\epsilon_{12}/dt$) as 0.054/second.

Once the evolution of PDF of shear stress (σ_{12}) is obtained, the evolution of mean, mode and standard deviations were calculated by standard operations on the PDF. The results are shown in Fig. 4. In particular, Fig. 4(a) shows the evolution (surface) of PDF of shear stress (σ_{12}) with time (t)/shear strain (ϵ_{12}). The evolution of PDF of shear stress is given in more detail in Fig. 4(b) showing contours of the PDF of shear stress (σ_{12}) and also the mean, mode, and standard deviations. The deterministic solution, obtained using the mean value of shear modulus (G) as fixed, deterministic input is also shown. As can be seen from Fig. 4(b), the standard deviation of shear stress increases in elastic regime (before approx. 0.056 s) until the yield point and then decreases as the solution approaches the critical state line. In other words, close to critical state the uncertainty in shear modulus (G) didn't have much effect on the uncertainty in shear stress as it had close to yielding. But on the other hand if one follows the evolution of deterministic solution one could see that even–though the deterministic solution coincides with mean and mode for pre-yield (elastic) behavior, it deviates for post-yield behavior, suggesting that the deterministic solution is neither the mean nor the most probable solution for post-yield response.

When compared with Monte–Carlo simulation, shown in Fig. 5, it can be seen that FPKE approach predicted the mean behavior exactly but it slightly over-predicted the standard deviation behavior. This difference is attributed to the approximation used to represent the

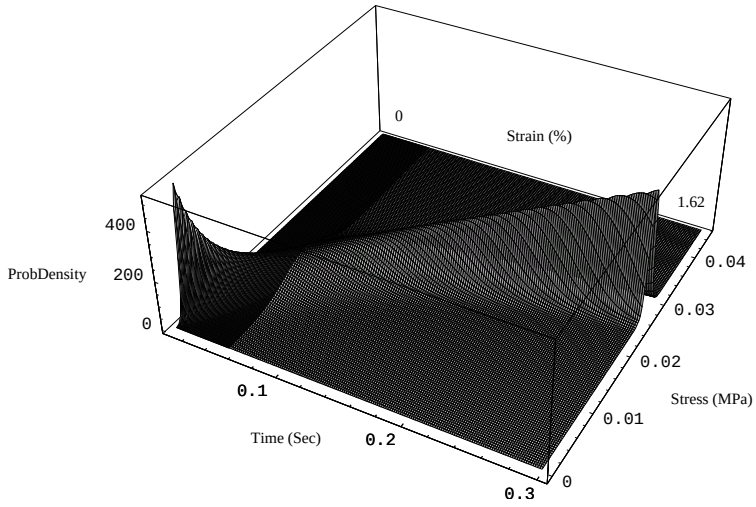

(a)

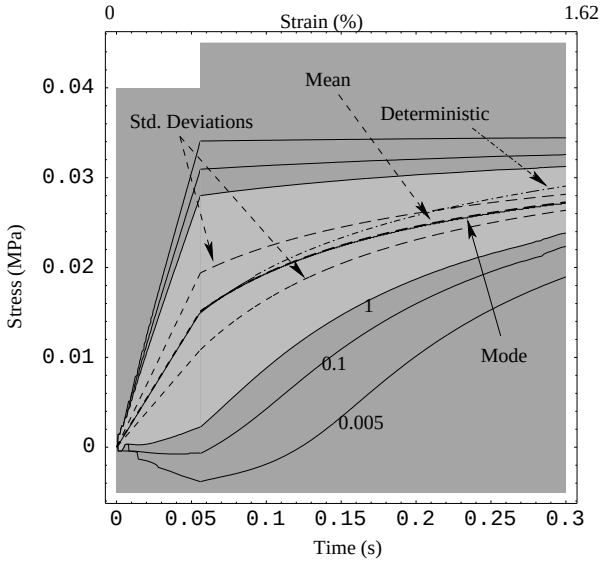

(b)

Figure 4. Low OCR Cam Clay Response with Random Normally Distributed Shear Modulus (G): (a) Evolution of PDF and (b) Evolution of Contours of PDF, Mean, Mode, Standard Deviations, and Deterministic Solution of Shear Stress (σ_{12}) with Time (t)/Shear Strain (ϵ_{12})

initial deterministic condition $\sigma_{12} = 0$ (Dirac delta function). One may note that at $\epsilon_{12} = 0$, the probability of shear stress (σ_{12}) at $\sigma_{12} = 0$ should theoretically be 1 i.e. all the probability mass should theoretically be concentrated at $\sigma_{12} = 0$ and would be best described by a Dirac delta condition. However, for numerical simulation of FPKE, that Dirac delta initial condition was approximated with a Gaussian function of mean zero and standard deviation of 0.00001 MPa as shown in Fig. 3. This initial error in standard deviation advected and diffused into the domain during the simulation of the evolution process. This error could be minimized by better approximating the Dirac delta initial condition (but at the expense of computational cost).

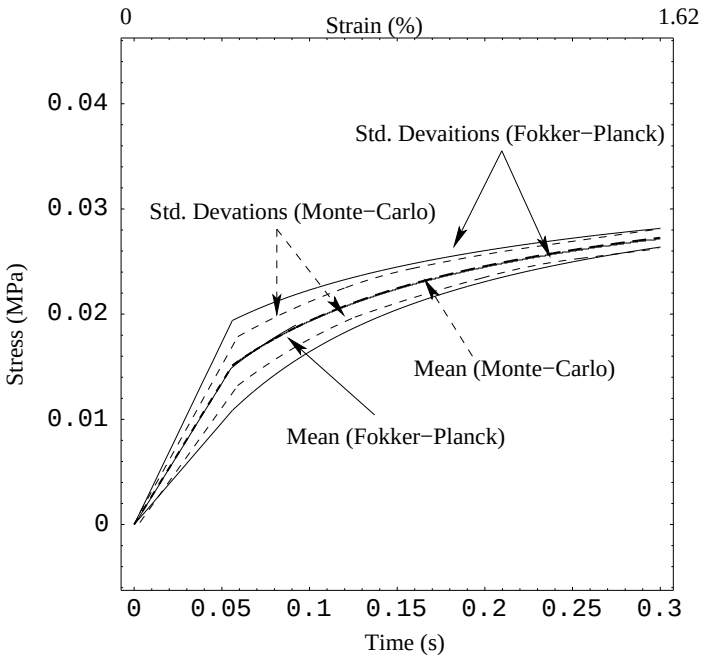

Figure 5. Comparison of FPK Approach and Monte–Carlo Approach for Low OCR Cam Clay Response with Random Normally Distributed Shear Modulus (G) in terms of Evolution of Mean and Standard Deviation of Shear Stress (σ_{12}) with Time (t)/Shear Strain (ϵ_{12})

Next few examples examine results (PDF of shear stress) by the introduction of uncertainties in other material parameters (other than shear modulus G). In examples where we use more than one random material property (see next examples) they are assumed uncorrelated and independent. The presented development can also deal with correlated random variables, as described by Fokker–Planck–Kolmogorov (FPK) equation 10. The advection and diffusion coefficients $N_{(1)}$ and $N_{(2)}$ (in Eq. (30)) will be changed accordingly for any correlation between random soil properties.

Additional uncertainty is introduced for the slope of critical state line M in terms of a normal distribution with mean value of 0.6 and a standard deviation of 0.1. The shear modulus G is again treated as random, as before. The resulting PDF of shear stress σ_{12} is now exhibiting a non-symmetric distribution in the post-yield (elastic–plastic) region. This non–symmetry is evident from different post-yield evolution of mean and mode of shear stress σ_{12} as seen in Fig. 6(b). The non–symmetry is also evident from the trace of the surface of PDF of shear stress at time $(t) = 0.3$s (or shear strain $(\epsilon_{12}) = 1.62\%$) in Fig. 6(a). Another interesting aspect to note (refer to Fig. 6(b)) is that for this assumed combination of material properties (random G and random M) the post-yield deterministic shear stress (σ_{12}) under-predicted the post-yield most probable (mode) shear stress (σ_{12}) but over-predicted the mean shear stress (σ_{12}).

The effect of addition of further uncertainty into the system, in terms of random normally distributed overconsolidation pressure (p_0) with a mean value of 0.2 MPa and standard deviation of 0.07 MPa, in addition to previously introduced random shear modulus (G) and random slope of critical state line (M), is shown in Fig. 7. It can be seen by comparing Figs. 6 and 7, the additional uncertainty in overconsolidation pressure (p_0) didn't affect much the

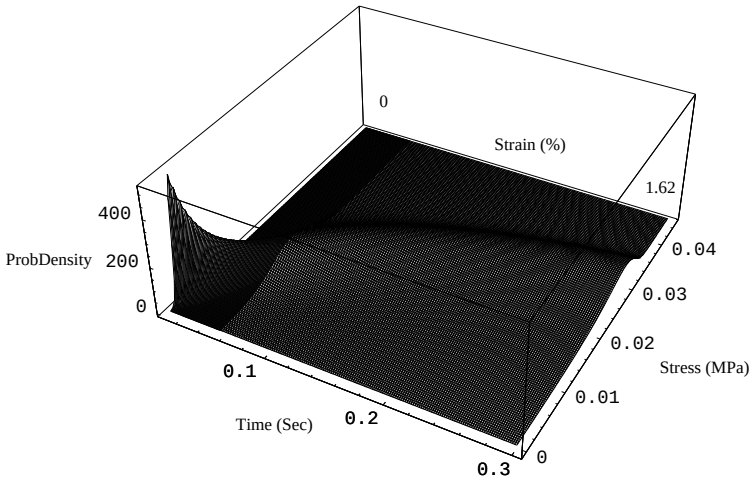

(a)

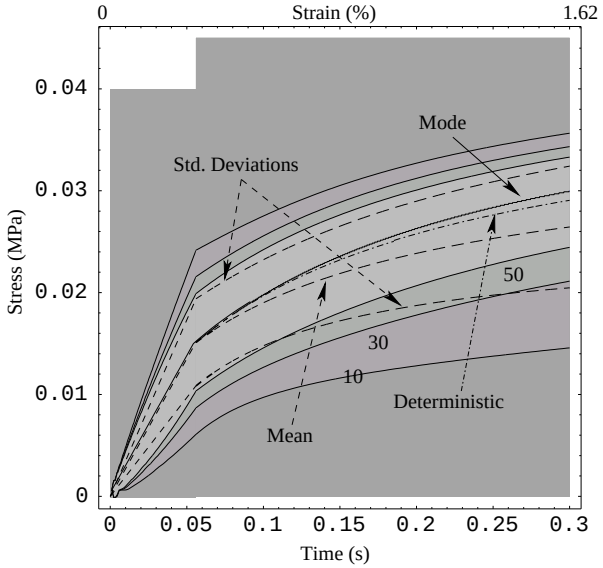

(b)

Figure 6. Low OCR Cam Clay Response with Random Normally Distributed Shear Modulus (G) and Random Normally Distributed Slope of Critical State Line (M): (a) Evolution of PDF and (b) Evolution of Contours of PDF, Mean, Mode, Standard Deviations, and Deterministic Solution of Shear Stress (σ_{12}) with Time (t) /Shear Strain (ϵ_{12})

probabilistic response of shear stress (σ_{12}) when compared to its response to random normally distributed shear modulus (G) and random normally distributed slope of critical state line (M) (Fig. 6). That is, the responses in Figs 6 and 7 are quite similar, at least qualitatively while quantitatively there are some small differences.

The uncertainty in overconsolidation pressure (p_0) didn't even have much effect on the probabilistic response (PDF) of shear stress (σ_{12}) when considered separately with random normally distributed shear modulus (G). This can be seen by comparing Fig. 8, where the probabilistic behavior of shear stress (σ_{12}) for low OCR cam clay model with randomly distributed shear modulus (G) and random normally distributed overconsolidation pressure (p_0) was presented, and Fig. 4. Similar to the case where the shear modulus was the only random parameter (Fig. 4), here also the post-yield deterministic shear stress (σ_{12}) overpredicted the post-yield mean and post-yield most probable (mode) shear stress (σ_{12}).

The probabilistic Cam–Clay elastic–plastic responses (low OCR) with different degrees of randomnesses (as presented above) were compared in Fig. 9. In that figure the PDFs of shear stress (σ_{12}) at shear strain (ϵ_{12}) $= 1.62\%$ are shown and compared with the deterministic value of shear stress obtained by choosing mean value (which in this case is also mode as we used normal distribution) of material properties. It is very interesting to note that the deterministic value of shear stress (σ_{12}) is different from the most probable (mode) value of shear stress (σ_{12}) for all the cases. It either under-predicted or over-predicted the most probable (mode) value.

Presented methodology is applicable to both hardening (as shown in examples above) and softening material response. A high OCR Cam–Clay material sample was analyzed. Following

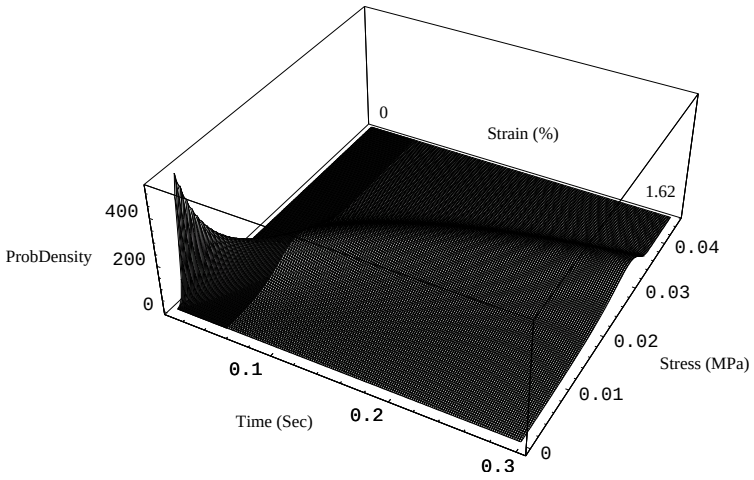

(a)

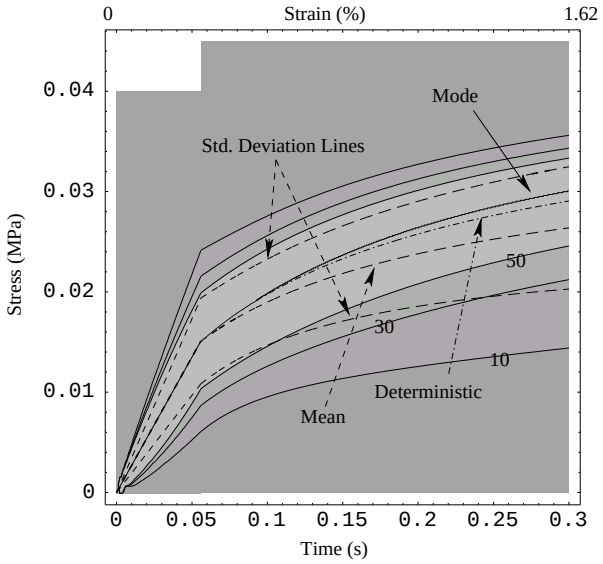

(b)

Figure 7. Low OCR Cam Clay Response with Random Normally Distributed Shear Modulus (G), Random Normally Distributed Slope of Critical State Line (M), and Random Normally Distributed Overconsolidation pressure (p_0): (a) Evolution of PDF and (b) Evolution of Contours of PDF, Mean, Mode, Standard Deviations, and Deterministic Solution of Shear Stress (σ_{12}) with Time (t)/Shear Strain (ϵ_{12})

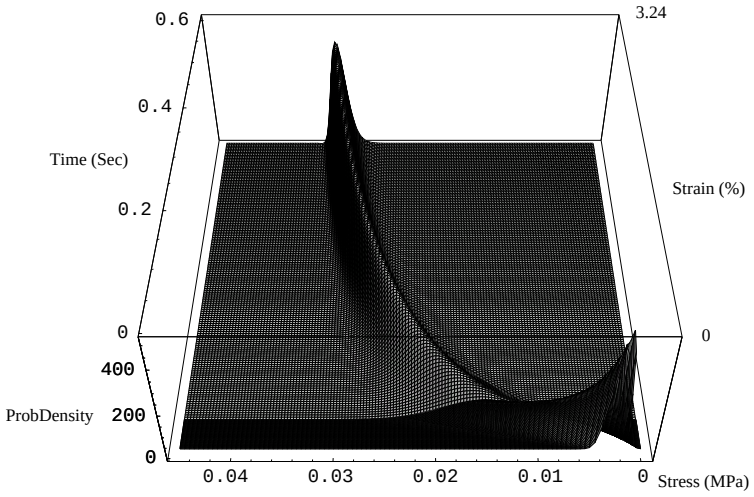

(a)

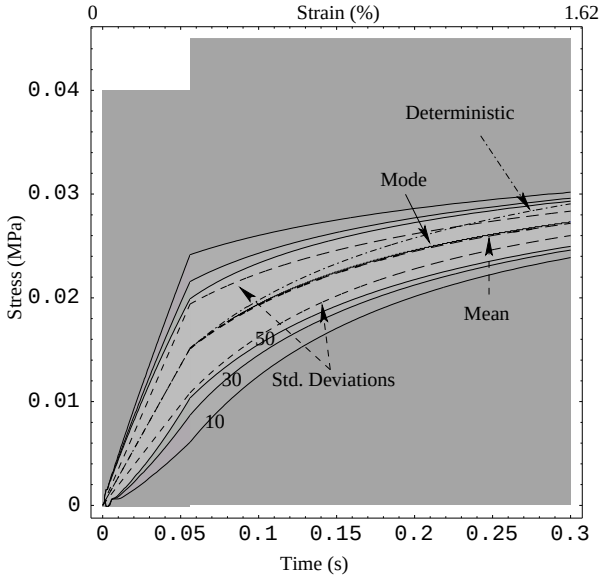

(b)

Figure 8. Low OCR Cam Clay Response with Random Normally Distributed Shear Modulus (G) and Random Normally Distributed Overconsolidation pressure (p_0): (a) Evolution of PDF and (b) Evolution of Contours of PDF, Mean, Mode, Standard Deviations, and Deterministic Solution of Shear Stress (σ_{12}) with Time (t)/Shear Strain (ϵ_{12})

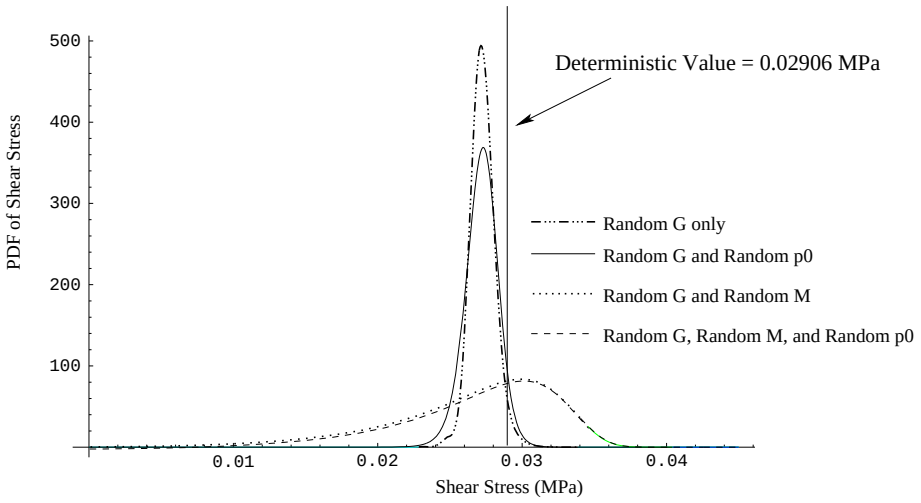

Figure 9. Comparison of Shear Stresses at 1.62% Shear Strain Obtained from Low OCR Cam Clay Model with different degrees of Randomnesses

parameters were used: random normally distributed shear modulus (G) with mean of 2.5 MPa and standard deviation of 0.5 MPa; random normally distributed slope of critical state line (M) with mean of 0.6 and standard deviation of 0.1; deterministic overconsolidation pressure $p_0 = 0.8$ MPa; deterministic applied confinement pressure $p = 0.02$ MPa; deterministic slopes of the unloading–reloading and normal compression lines in $e - \ln(p')$ space $\kappa = 0.05$ and $\lambda = 0.25$, respectively; deterministic initial void ratio $e_0 = 2.18$. The (arbitrary) value of strain rate is still the same, $d\epsilon_{12}/dt = 0.054$/s. The resulting PDF of shear stress is shown in Fig. 10(a). Fig. 10(b) gives a more detailed view of results, in terms of evolution of contours of PDF, mean, mode, standard deviation and deterministic solution of shear stress (σ_{12}). Similar to the low OCR simulation with random G and random M, the high OCR simulation also yielded a symmetric distribution of PDF shear stress (σ_{12}) in the pre-yield (elastic) regime and a non-symmetric distribution of PDF shear stress (σ_{12}) in the post-yield (elastic-plastic)

regime. Similarly to probabilistic response for low OCR (with random G and random M), the deterministic shear stress (σ_{12}) coincided with the mean and most probable (mode) shear stress in the pre-yield (elastic) regime but deviated in the post-yield non-linear elastic-plastic regime. The deterministic shear stress (σ_{12}) under-predicted the mean shear stress (σ_{12}) in the entire post-yield regime but over-predicted the most probable (mode) shear stress (σ_{12}) in the region close to the yield point, though close to critical state line it under-predicted the most probable (mode) shear stress (σ_{12}).

Verification of probabilistic simulations for high OCR sample were again done using Monte–Carlo approach. Fig 11 compares the evolution of mean and standard deviation of shear stress (σ_{12}) obtained using FPKE approach and Monte–Carlo approach. It can be seen that FPKE approach slightly overpredicted the standard deviation behavior because of the reasons discussed earlier. That is, the FPKE approach is somewhat "wider" since the initial condition was not a Dirac delta function, but rather an approximation. Again, this deviation in initial condition (from Dirac delta function) can be controlled by choosing an initial normal distribution for PDF of shear stress with smaller standard deviation, but this will increase computational cost in solving the resulting finite difference system of equations.

6. CONCLUSIONS

In this paper we presented methodology to solve the probabilistic elastic–plastic differential equations. The methodology is based on Eulerian–Lagrangian form of the Fokker–Planck–Kolmogorov equation and provides for full description of the probability density function (PDF) of stress response for given strain. Of particular interest was the modeling of stress–strain constitutive response for materials with uncertain material parameters. These

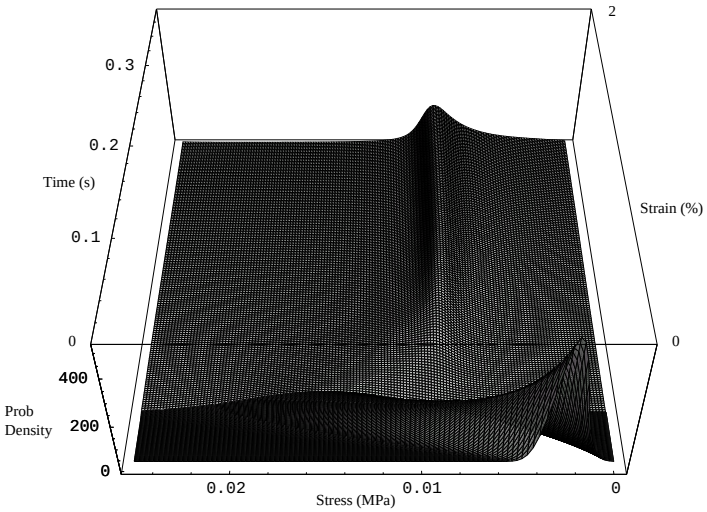

(a)

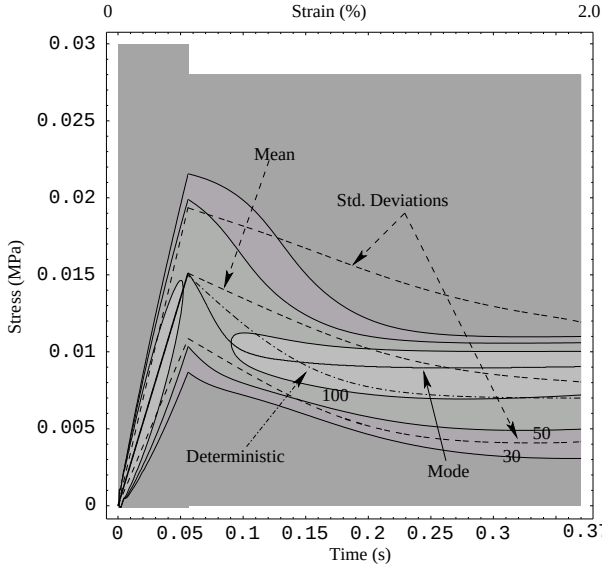

(b)

Figure 10. High OCR Cam Clay Response with Random Normally Distributed Shear Modulus (G) and Random Normally Distributed Slope of Critical State Line (M): (a) Evolution of PDF and (b) Evolution of Contours of PDF, Mean, Mode, Standard Deviations, and Deterministic Solution of Shear Stress (σ_{12}) with Time (t) /Shear Strain (ϵ_{12})

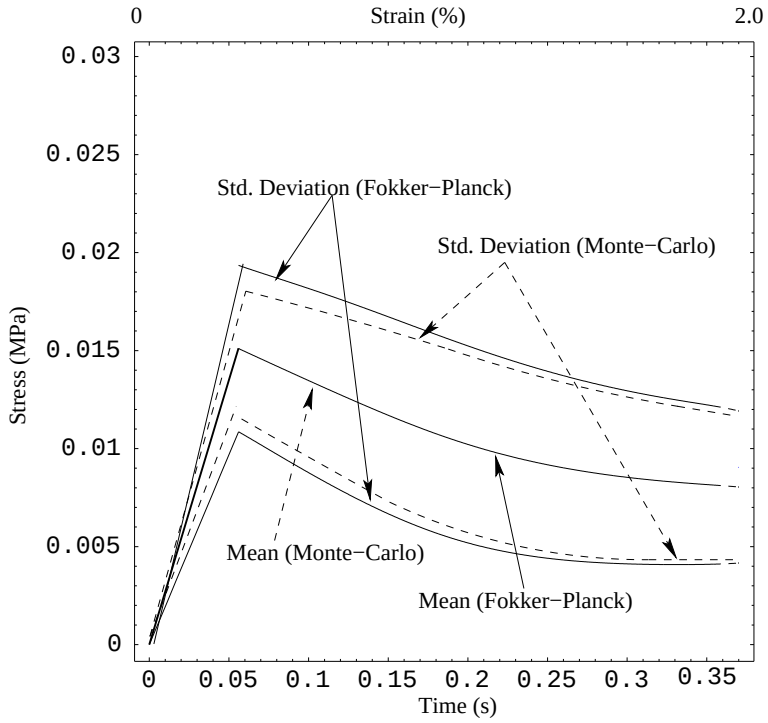

Figure 11. Comparison of FPK Approach and Monte–Carlo Approach for High OCR Cam Clay Response with Random Normally Distributed Shear Modulus (G) and Random Normally Distributed Slope of Critical State Line (M) in terms of Evolution of Mean and Standard Deviation of Shear Stress (σ_{12}) with Time (t)/Shear Strain (ϵ_{12})

uncertainties in material properties are present in most materials, and it is just our simplification to a single value (say mean) that renders deterministic properties usually used for simulations The effects of nonlinear hardening/softening on predicted PDF of stress were investigated in some more detail. It was shown that the nonlinear hardening/softening creates a discrepancy between the most likely stress solution and the deterministic solution, meaning that the usually obtained deterministic solution is not the most likely outcome of a constitutive stress-strain simulation if material paramaters are uncertain.

REFERENCES

1. Maciej Anders and Muneo Hori. Stochastic finite element method for elasto-plastic body. *International Journal for Numerical Methods in Engineering*, 46:1897–1916, 1999.
2. Gregory B. Baecher and John T. Christian. *Reliability and Statistics in Geotechnical Engineering*. Wiley, West Sussex PO19 8SQ, England, second edition, 2003. ISBN 0-471-49833-5.
3. Ronaldo I. Borja. Incorporating uncertainties in nonlinear soil properties into numerical models. In *Proceedings of International Workshop on Uncertainties in Nonlinear Soil Properties and their Impact on Modeling Dynamic Soil Response, PEER Headquarters, UC Berkeley, March 18-19, 2004*, Opinion Paper, http://peer.berkeley.edu/lifelines/Workshop304/pdf/o_Borja.pdf, 2004. PEER.
4. J. M. Duncan. Factors of safety and reliability in geotechnical engineering. *ASCE Journal of Geotechnical and Geoenvironmental Engineering*, 126(4):307–316, April 2000.
5. Gordon A. Fenton. Estimation of stochastic soil models. *Journal of Geotechnical and Geoenvironmental Engineering*, 125(6):470–485, June 1999.
6. Gordon A. Fenton. Random field modeling of cpt data. *Journal of Geotechnical and Geoenvironmental Engineering*, 125(6):486–498, June 1999.
7. Gordon A. Fenton and D. V. Griffiths. Three-dimensional probabilistic foundation settlement. *Journal of Geotechnical and Geoenvironmental Engineering*, 131(2):232–239, February 2005.
8. C. W. Gardiner. *Handbook of Stochastic Methods for Physics, Chemistry and the Natural Science*. Springer:Complexity. Springer-Verlag, Berlin Heidelberg, third edition, 2004.
9. Roger G. Ghanem and Pol D. Spanos. *Stochastic Finite Elements: A Spectral Approach*. Dover Publications, Inc., Mineola, New York, 2003.
10. Boris Jeremić, Kallol Sett, and M. Levent Kavvas. Probabilistic elasto-plasticity: Formulation of evolution equation of probability density function. *Journal of Engineering Mechanics*, (to appear), 2005.
11. M. Levent Kavvas. Nonlinear hydrologic processes: Conservation equations for determining their means and probability distributions. *Journal of Hydrologic Engineering*, 8(2):44–53, March 2003.
12. R. Kubo. Stochastic liouville equations. *J. Math. Phys.*, 4(2):174–183, 1963.
13. Hermann G. Matthies and Andreas Keese. Galerkin methods for linear and nonlinear elliptic stochastic partial differential equations. *Computational Methods in Applied Mechanics and Engineering*, 194(1):1295–1331, April 2005.
14. William L. Oberkampf, Timothy G. Trucano, and Charles Hirsch. Verification, validation and predictive

capability in computational engineering and physics. In *Proceedings of the Foundations for Verification and Validation on the 21st Century Workshop*, pages 1–74, Laurel, Maryland, October 22-23 2002. Johns Hopkins University / Applied Physics Laboratory.

15. Kok-Kwang Phoon and Fred H. Kulhawy. Characterization of geotechnical variability. *Canadian Geotechnical Journal*, 36:612–624, 1999.
16. Kok-Kwang Phoon and Fred H. Kulhawy. Evaluation of geotechnical property variability. *Canadian Geotechnical Journal*, 36:625–639, 1999.
17. J. B. Roberts and P. D. Spanos. Stochastic averaging: An approximate method of solving random vibration problems. *International Journal of Non-Linear Mechanics*, 21(2):111–134, 1986.
18. Kallol Sett, Boris Jeremić, and M. Levent Kavvas. Probabilistic elasto-plasticity: Solution and verification of evolution equation of probability density function. *Journal of Engineering Mechanics*, (to appear), 2005.
19. C. Soize. *The Fokker-Planck Equation for stochastic dynamical systems and its explicit steady state solutions*. World Scientific, Singapore, 1994.
20. K. H. Stokoe II, R. B. Darendeli, R. B. Gilbert, F.-Y. Menq, and W. K. Choi. Development of a new family of normalized modulus reduction and material damping curves. In *International Workshop on Uncertainties in Nonlinear Soil Properties and their Impact on Modeling Dynamic Soil Response, PEER Headquarters, UC Berkeley, March 18-19, 2004*, Plenary Paper, http://peer.berkeley.edu/lifelines/Workshop304/pdf/Stokoe_PlenaryPaper.pdf. PEER.
21. B. Sudret and A. Der Kiureghian. Stochastic finite element methods and reliability: A state of the art report. Technical Report UCB/SEMM-2000/08, University of California, Berkeley, 2000.
22. N. G. Van Kampen. Stochastic differential equations. *Phys. Rep.*, 24:171–228, 1976.
23. Stephen Wolfram. *Mathematica: A System for Doing Mathematics by Computer*. Addison-Wesley, Redwood City, second edition, 1991.
24. W. Q. Zhu, J. S. Yu, and Y. K. Lin. On improved stochastic averaging procedure. *Probabilistic Engineering Mechanics*, 9(3):203–211, 1994.

APPENDIX

NOTATION

This is a summary of notations used in mathematical derivations:

D_{ijkl}: Material parameter tensor, function of D^{el}_{ijkl}, f, U, q_*, and r_*,

D^{el}_{ijkl}: Elastic stiffness tensor,

D^{ep}_{ijkl}: Elastic–plastic tangent stiffness tensor,

σ_{ij}: Cauchy stress tensor, in indicial notation,

e: Void ratio of soil,

e_0: Initial void ratio of soil,

f: Yield surface,

G: Shear modulus of soil,

K: Bulk modulus of soil,

K_P: Plastic modulus,

C_{ijm}: Coefficient tensor in multivariate Itô equation, in indicial notation,

M: Slope of critical state line in $p - q$ space,

$N_{(1)}$: Advection coefficient of FPK equation,

$N_{(2)}$: Diffusion coefficient of FPK equation,

$P(\cdot, t)$: Probability density at time, t,

p: first invariant of stress tensor,

p_0: Hydrostatic pressure, the soil under analysis has experienced before (internal variable in Cam Clay model),

$\bar{p}_0$: Direction of evolution of p_0,

q: Invariant of stress tensor, equal to $\sqrt{\frac{3}{2}s_{ij}s_{ij}}$

q_*: Internal variables,

r_*: Directions of evolution of internal variables,

s_{ij}: second invariant of the deviatoric stress tensor,

t, t_1, t_2: time,

U: Potential surface,

W_i: Increment of vector Wiener process,

x_t: Spatial location at time, t,

ϵ_{kl}: Strain tensor,

$\dot{\epsilon}$: Strain rate,

λ: Slope of normal consolidation line in $e - ln(p)$ space,

κ: Slope of unloading-reloading line in $e - ln(p)$ space,

η_{ij}: Spatial-temporal operator tensor, function of σ_{ij}, D_{ijkl}, and ϵ_{kl},

$\rho(\cdot, t)$: Phase density at time, t,

τ: time,

ζ: Probability current